Cell. Mol. Life Sci. 66 (2009) 1766 – 1781
1420-682X/09/101766-16
DOI 10.1007/s00018-009-9169-4

Cellular and Molecular Life Sciences

Research Article

PPAR γ partial agonist, KR-62776, inhibits adipocyte differentiation via activation of ERK

J. Kim[a], D. C. Han[a], J. M. Kim[a], S. Y. Lee[a], S. J. Kim[a], J. R. Woo[a], J. W. Lee [a], S.-K. Jung[a], K. S. Yoon[a], H. G. Cheon[b], S. S. Kim[b], S. H. Hong[c] and B.-M. Kwon[a, *]

[a] Laboratory of Chemical Biology and Genomics, Korea Research Institute of Bioscience and Biotechnology, and University of Science and Technology in Korea, 52 Uendong Yoosung Daejon 305 – 600 (Korea), Fax: +82-861-2675, e-mail: kwonbm@kribb.re.kr
[b] Korea Research Institute of Chemical Technology, Daejon 305 – 343 (Korea)
[c] Department of Dental Microbiology, Kyungpook National University School of Dentistry, Daegu 700 – 412 (Korea)

Received 04 March 2009; received after revision 13 March 2009; accepted 17 March 2009
Online First 7 April 2009

Abstract. Indenone KR-62776 acts as an agonist of PPARγ without inducing obesity in animal models and cells. X-ray crystallography reveals that the indenone occupies the binding pocket in a different manner than rosiglitazone. 2-Dimensional gel-electrophoresis showed that the expression of 42 proteins was altered more than 2.0-fold between KR-62776- or rosiglitazone-treated adipocyte cells and control cells. Rosiglitazone down-regulated the expression of ERK1/2 and suppressed the phosphorylation of ERK1/2 in these cells. However, the expression of ERK1/2 was up-regulated in KR-62776-treated cells. Phosphorylated ERK1/2, activated by indenone, affects the localization of PPARγ, suggesting a mechanism for indenone-inhibition of adipogenesis in 3T3-L1 preadipocyte cells. The preadipocyte cells are treated with ERK1/2 inhibitor PD98059, a large amount of the cells are converted to adipocyte cells. These results support the conclusion that the localization of PPARγ is one of the key factors explaining the biological responses of the ligands.

Keywords. Peroxisome proliferators-activated receptor γ, rosiglitazone, adipocyte, lipolysis, ERK, indenone.

Introduction

Type II diabetes mellitus (T2DM) is characterized by abnormal glucose homeostasis leading to hyperglycemia. Its pathogenesis is caused by complex interactions between genetic and environmental factors [1]. Peroxisome proliferator-activated receptor γ (PPARγ) is a member of the nuclear hormone receptor superfamily. PPARγ, predominantly expressed in adipose tissue and myeloid cells, has been demonstrated to regulate adipocyte differentiation and inflammatory responses [2, 3]. PPARγ is recognized as a target protein for anti-diabetic drugs, and glitazones (TZD) such as rosiglitazone (RGZ), troglitazone, and pioglitazone were developed as PPARγ agonists [4]. They increase insulin-stimulated glucose uptake and utilization in both animal models and human subjects [5, 6].
Rosiglitazone (RGZ), one of the TZD drugs, is widely used as an anti-diabetic medicine for patients with type 2 diabetes or non-insulin dependent diabetes (NIDDM). Rosiglitazone helps to lower blood sugar

* Corresponding author.

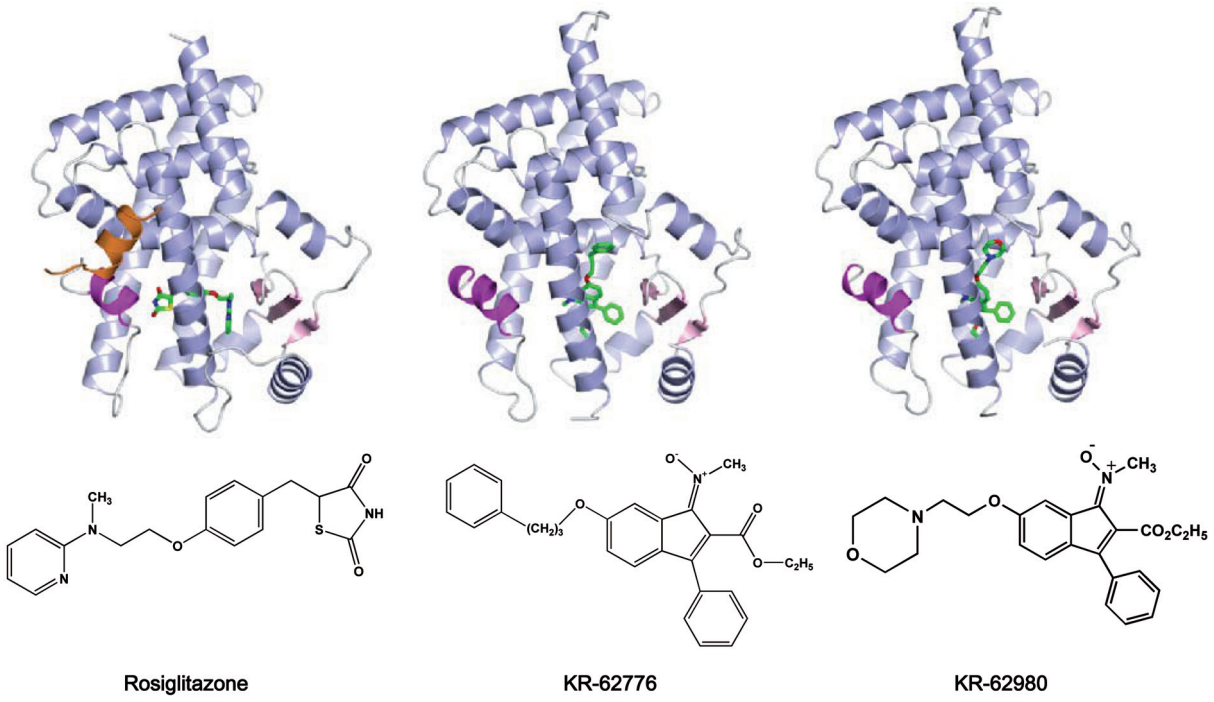

Figure 1. Structure of peroxisome proliferator-activated receptor γ (PPARγ) agonists, KR-62776, KR-62980 and rosiglitazone. A comparison of the ligand binding pattern of PPARγ with KR62980 (right), KR62776 (center) and rosiglitazone (left).

levels by increasing the sensitivity of liver, fat and muscle cells to insulin. Rosiglitazone also preserves the function of the pancreatic β cells that produce insulin [7]. Therefore, rosiglitazone controls the sugar level in blood and helps prevent diabetic diseases. However, it does have side effects that include obesity and liver toxicity [8]. During the development of novel and PPARγ-specific agonists that inhibit adipocyte differentiation but stimulate insulin-mediated glucose uptake in adipocytes, we found a new type of PPARγ-specific agonist, indenones such as KR-62776 and KR-62980 [9, 10]. These agonists, shown in Figure 1, are structurally distinct from the glitazones. KR-62776 acts as a selective PPARγ agonist in a transactivation assay with an EC_{50} of 50 nM [9]. In fully differentiated 3T3-L1 adipocytes, KR-62776 induces [^{3}H]-deoxyglucose uptake in a concentration-dependent manner regardless of insulin stimulation; GLUT4 translocation to the plasma membrane was observed concomitantly. KR-62980 also activates PPARγ in the transactivation assay in a dose-dependent manner with an EC_{50} of 15 nM. Treatment of C57BL6J mice with KR-62980 for 14 days (50 mg/kg, bid) reduces plasma glucose levels. Therefore, KR-62980 is a PPARγ agonist with anti-diabetic effects. One interesting point is that the indenones do not induce weight gain in animal tests [10].

Willson et al. reported that the PPARγ ligand GW0072 inhibits adipocyte differentiation in cell culture. This may be because GW0072 occupies a different binding site within the ligand-binding pocket than the known PPARγ agonists [11]. X-ray crystallography also confirmed that KR-62776 and KR-62980 utilize a different binding pocket of PPARγ than the known PPARγ agonists. In addition, PPARγ antagonists, such as bisphenol A diglycidyl ether (BADGE) and LG100641, possess antiobesity and antidiabetic activity because they inhibit adipocyte differentiation and stimulate glucose uptake in 3T3-L1 adipocytes [12, 13].

PPARγ is one of the nuclear receptors shown to function both in the nucleus and in the cytoplasm. The adipogenic and transcriptional activity of PPARγ was modulated upon mitogenic stimulation due to phosphorylation of its Ser84 by ERKs [14]. The localization of PPARγ is mediated by direct MEK-PPARγ interaction. Mitogenic stimulation of the cells induces interaction between active nuclear MEK and PPARγ, followed by a rapid nuclear export of PPARγ, and a reduction in the transcriptional activity of PPARγ. Therefore, the ERK-activator MEK modulates activity of PPARγ through regulation of its subcellular localization [15].

To unveil the cellular regulatory mechanism of the PPARγ agonists, we compared proteomic profiles in KR-62776- or rosiglitazone-treated 3T3-L1 adipocytes. Proteins regulated by the PPARγ agonists were separated by two-dimensional gel electropho-

resis and identified by delayed extraction-matrix assisted laser desorption ionization-time of flight mass spectrometry (DE-MALDI-TOF MS). We also analyzed the molecular alterations stimulated by both KR-62776 and rosiglitazone in 3T3-L1 preadipocyte cells to identify potential molecular therapeutic targets associated with obesity or diabetes.

Materials and methods

Cell culture and treatment. 3T3-L1 (ATCC CL-173) preadipocyte cells were grown on 150 mm dishes in Dulbecco modified Eagle Medium (DMEM) with 10% fetal bovine serum (FBS) at 37 °C in 5% CO_2. 3T3-L1 preadipocyte cells were stimulated to undergo differentiation with 3-isobutyl-1-methylxanthine (0.5 mM), dexamethasone (1 μM) and insulin (200 nM) for seven days. Cell differentiation was monitored by phase-contrast microscopy. Rosiglitazone or KR-62776 was added at a concentration of 1 μM. Confluent 3T3-L1 preadipocyte cells were incubated with 1 μM rosiglitazone or KR-62776 in the presence of 200 nM insulin, with a medium change every 2 – 3 days. After 7 – 9 days of differentiation, the cells were harvested, and the lysates were aliquoted and stored at -70 °C.

X-ray crystal structure. PPARγ LBD, in complex with indenone compounds KR62776, was crystallized as previously described with slight modifications [16]. Briefly, purified PPARγ LBD was incubated overnight with 10 mM of either KR62980 or KR62776 compound, 10% (v/v) DMSO, 20 mM HEPES buffer (pH 7.5) and 100 mM NaCl and then concentrated to 10 mg/ml. Crystals were grown by mixing 1.8 μl of protein solution and equal volume of reservoir solution containing 3.4 M sodium formate, 0.05 M Tris/HCl buffer, 1% (v/v) PEG 6K, 5% (v/v) DMSO and 10 mM of desired compound. X-ray diffraction data were collected on beamline 6B of the Pohang Accelerator Laboratory (PAL). The collected data were scaled and processed using the programs MOSFLM and SCALA in the CCP4 suite. The structure was determined by molecular replacement method using the Ligand Binding Domain (LBD) structure of PPARγ (PDB code: 3PRG) as a search model. The program EPMR placed one LBD of PPARγ in the asymmetric unit. Refinement was carried out using the program CNS. A randomly selected 5% of data were set aside for the R_{free} calculation. Rounds of refinements were performed with manual rebuilding by using the program [17, 18].

Oil-Red O staining. The Oil-Red O staining method is a modification of a published protocol [19]. 3T3-L1 cells in 24-well plates were incubated with 10% formaldehyde in PBS for 5 min at room temperature. Fixation of the cell was continued by incubation for longer than 1 h at 4 °C with 10% formaldehyde after replacing the previous solution. A stock solution of Oil-Red O (0.5 g in 100 mL isopropanol) was prepared and passed through a 0.2 μm filter. To prepare the working solution, 6 mL of the stock solution was mixed with 4 mL of distilled water, left for 20 min at room temperature, and filtered through a 0.2 μm filter prior to use. The fixing solution was discarded and Oil-Red O working solution was added to the fixed cells for 15 min at room temperature. The wells were rinsed four times with 500 μL of distilled water and pictures were taken. The dye retained by the cells was eluted by incubation with 100 μL isopropanol. The OD_{540} was measured using a Bio-Rad model 680 microplate reader. The absorbance of the blank was determined using isopropanol eluted from an empty well stained as previously described.

Two-dimensional gel electrophoresis. IEF (isoelectric focusing) was carried out using the commercially available, dedicated apparatus, Protean IEF Cell (Bio-Rad). IPG strips were used according to the reported method [20] and the manufacturer's instructions. Samples containing up to 150 μg of protein for analytical gels or up to 1 mg for micropreparative gels, were diluted to 400 μL with rehydration solution (7 M urea, 2 M thiourea, 2% CHAPS, 100 mM DTT, 0.5% (v/v) pH 3–10 IPG buffer, trace bromophenol blue), and applied to strips by overnight rehydration at 50 V. Proteins were focused successfully for 15 min at 250 V, then a gradient was applied from 250 to 10 000 V in 3 h. Focusing was continued at 10 000 V for 6 h to give a total of 60 kVh on the Protean IEF Cell. All IEF steps were carried out at 20 °C. After the first-dimensional IEF, IPG gel strips were placed in an equilibration solution (6 M urea, 2% SDS, 30% glycerol, 50 mM Tris-HCl, pH 8.8) containing 2% DTT for 10 min with shaking at 45 rpm on an orbital shaker. The gels were then transferred to the equilibration solution containing 2.5% iodoacetamide and shaken for a further 10 min before placing them on an 8% polyacrylamide gel slab (185 x 200 x 1.0 mm). Separation in the second dimension was carried out using Protean II xi electrophoresis equipment and Tris-glycine buffer (25 mM Tris, 192 mM glycine) containing 0.1% SDS, at a current setting of 5 mA/gel for the initial 1 h and 10 mA/gel thereafter. The second dimension SDS-PAGE was continued until the bromophenol blue dye marker had reached the bottom of the gel.

Protein visualization and image analysis. For silver staining, following second-dimension SDS-PAGE, analytical gels were immersed in a solution of methanol: acetic acid: water (50:12:38) for 1.5 h, followed by washing twice in 50 % ethanol for 20 min. Gels were pretreated for 1 min in a solution of 0.02 % $Na_2S_2O_3$. This was followed by three 1-min washes in deionized water. Proteins were stained in a solution containing 0.2 % $AgNO_3$ and 0.075 % (v/v) formalin (37 % formaldehyde in water) for 20 min and washed twice in deionized water for 1 min. Subsequently, gels were developed in a solution of 0.06 % (v/v) formalin, 2 % Na_2CO_3, and 0.0004 % $Na_2S_2O_3$. When the desired intensity was attained, the developer was discarded and stopped by 1 % acetic acid.

For Coomassie blue staining of micropreparative gels, gels were washed three times in deionized water for 10 min. Gels were then stained in a solution containing 34 % methanol, 3 % phosphoric acid, 10 % ammonium sulfate and 0.1 % Coomassie Brilliant Blue G-250. Staining was carried out overnight. Protein patterns in the gels were recorded as digitized images using a high resolution scanner (GS-800 Calibrated Imaging Densitometer, Bio-Rad). Gel image matching was done with PDQuest software (version 7.1.0; Bio-Rad). Scanned gel images were processed to remove background, staining on the gel borders and to automatically detect spots. For all spot intensity calculations, normalized values were used. Normalization of spot intensity was done so that the total sum of intensities in a gel would be equal to 1 000 000, where normalized spot intensities were expressed in ppm.

In-gel digestion. In-gel digestion of protein spots from Coomassie-stained gels were performed following a known method [21]. After the completion of staining, the gel slab was washed twice with water for 10 min. Spots of interest were excised with a scalpel, cut into pieces, and put into 1.5 mL microtubes. The particles were washed three times with water/acetonitrile (1:1, v/v) for 15 min until the coomassie brilliant blue dye was removed from the gel.

The solvent volumes were about twice the gel volume. The liquid was removed and the particles were rehydrated in 0.1 M NH_4HCO_3 for 5 min. Acetonitrile was added to give a 1:1 (v/v) mixture of 0.1 M NH_4HCO_3/acetonitrile and the mixture was incubated for 15 min. The liquid was removed and gel particles were dried in a vacuum centrifuge (Heto, MAXY-Dry Lyo Vacuum Concentration System, UK), rehydrated in 10 mM DTT/0.1 M NH_4HCO_3, and incubated for 45 min at 56 °C to reduce the peptides. After cooling the tubes to room temperature and removing the liquid, 55 mM iodoacetamide in 0.1 M NH_4HCO_3 was added. The tubes were incubated for 30 min at room temperature in the dark to S-alkylate the peptides. Iodoacetamide solution was removed, the gel particles were washed with 0.1 M NH_4HCO_3 and acetonitrile. The samples were dried in a vacuum centrifuge, rehydrated on ice in digestion buffer containing 50 mM NH_4HCO_3 and 12.5 ng/μL of trypsin, and incubated for 45 min on ice. Excess liquid was removed and about 10 μL of digestion buffer without trypsin was added. Following overnight digestion at 37 °C, 10 % trifluoroacetic acid was added and the supernatant was recovered. 0.1 % trifluoroacetic acid/60 % acetonitrile was added and the tube was incubated for 30 min. The supernatant was recovered, and this step was repeated twice. The total extracts were pooled and dried in a vacuum centrifuge.

Zip tip C18 purification for MS. The dried extract was reconstituted in 10 μL of deionized water. A reverse-phase ZipTip C18 microcolumn (Millipore, Villerica, MA. USA; 15 μm tip, coated with spherical silica-based C18 resin for peptide concentration, desalting, and fractionation) was pre-equilibrated with 100 % acetonitrile followed by 50 % acetonitrile before washing with 0.1 % trifluoroacetic acid. The reconstituted sample was drawn into the tip to allow peptide binding, and was then washed three times with 10 μL of 0.1 % trifluoroacetic acid to remove any contaminants that might interfere with matrix-peptide cocrystallization and/or peptide ionization. The peptides were eluted with 10 μL of 50 % acetonitrile in 0.1 % trifluoroacetic acid solution three times and the eluted solutions were dried in a vacuum centrifuge.

MALDI-TOF MS and database search. Tryptic peptides were analyzed in a Voyager-DE STR MALDI-TOF mass spectrometer (Applied Biosystems, Foster City, CA, USA). The spectrometer was run in positive ion mode and in reflector mode with the following settings: accelerating voltage, 20 kV; grid voltage, 76 %; guide wire voltage, 0.01 %; and a delay of 150 ns. The low mass gate was set at 800 m/z. Proteins were identified by peptide mass fingerprinting with the search programs MS-FIT (http://prospector.ucsf.edu/prospector/4.0.8/html/msfit.htm). The following search parameters were applied: SWISS-PROT and NCBI were used as the protein sequence databases; a mass tolerance of 50 ppm and one incomplete cleavage were allowed; acetylation of the N-terminus, alkylation of cysteine by carbamidomethylation, oxidation of methionine, and pyroGlu formation of N-terminal Gln were considered as possible modifications. The proteins were considered as correctly identified when both softwares gave the same identification with a p value <0.005 and at least 20 % coverage of the sequence.

Western blot analysis. The 3T3-L1 cell lysates were prepared by incubating cells in an ice-cold RIPA buffer (40 mM Tris-HCl, pH 7.5, 150 mM NaCl, 0.1 % SDS, 0.5 % sodium deoxycholate, 1 % Triton X-100, 0.1 mM EDTA, 1 mM sodium vanadate, and Complete™ protease inhibitor cocktail). The cell lysates were clarified by centrifugation at 20 000 *g* for 20 min at 4 °C. Protein concentrations of the lysates were determined using BSA as a standard control with the Bio-Rad^{DC} protein assay kit. Twenty micrograms of protein were loaded onto 10 % SDS-polyacrylamide gels, transferred onto a PVDF membrane, and blocked with Western blocking solution in TTBS (10 mM Tris-HCl, pH 7.6, 150 mM NaCl, and 0.05 % Tween 20) at room temperature for 1 h. The blots were incubated with primary antibody for 2 h, washed three times, incubated with secondary antibodies for 1 h, and washed an additional three times. Specific antibody signals were detected with an enhanced chemiluminescence (ECL) detection system (Roche, Indianapolis, IN, USA). The following antibodies were used in this study: anti-PPARγ (Santa Cruz; sc-7273), anti-phospho-PPARγ [Ser112] (chemicon; MAB3632), anti-Phospho-p44/42 Map kinase [Thr202/Tyr204] (Cell Signaling; #9101), anti-MEK1/2 [47E6] (Cell Signaling; #9126), anti-p44/42 MAP kinase (Cell Signaling; #9102), anti-ERK 1 [K-23] (Santa Cruz; sc-94), anti-Histone H1 (Santa Cruz;8030), anti-GAPDH (Ab frontier; #LF-PA0018), anti-β-Actin (sigma;A5316) HRP-conjugated goat anti-rabbit IgG [H+L] (Jackson Immunoresearch;115-035-062), and HRP-conjugated goat anti-rabbit IgG [H+L] (Jackson Immunoresearch;112-035-045).

Immunofluorescence in 3T3-L1 cells. For all immunofluorescence experiments, cells were grown on coverslips. Cell were fixed with 4 % (wt/vol) paraformaldehyde in PBS and then permeabilized for 5 min with 0.2 % Triton X-100 in PBS. The cells were incubated with antibodies directed against PPARγ (Santa Cruz Biotechnology, Inc.), ERK1 (Santa Cruz Biotechnology, Inc.), and MEK1 (Cell Signaling) for 2 h at room temperature. Preparations were then incubated with a combination of Texas Red-conjugated anti-mouse IgG and fluorescein isothiocyanate-conjugated anti-rabbit IgG (Santa Cruz Biotechonology). Nuclei were visualized following a 5 min incubation with 0.2 mg/ml 4',6'-diamidino-2-phenyl-indole (DAPI). Slides were photographed using a digital camera-connected epifluorescence microscope.

Nuclear and cytosolic fractionation. The preparation of nuclear and cytosolic fractions was modified from the procedure described by Meunier et al. [22]. Briefly, postconfluent 3T3-L1 preadipocytes were incubated in DMEM culture medium containing 200 nM insulin with DMSO, 1 μM KR-62776 or 1 μM RGZ for nine days. Then the cells were washed with cold PBS, suspended in ice-cold buffer F (210 mM mannitol, 70 mM sucrose 5 mM Tris, pH 7.5, 1 mM EDTA, supplemented with protease inhibitors) left in the buffer for 15 minutes on ice and then dounce homogenized (15 strokes). The nuclei were separated by centrifugation (500 *g*, 5 minutes, 4 °C). The supernatant, containing the cytosolic fraction, was saved and the pellet, containing the nuclei, was washed with PBS and resuspended in RIPA buffer for 5 min on ice, centrifuged again and the nuclear fraction moved into the supernatant. Statistical analysis was performed using a two-tailed Student's *t*-test, and $p < 0.05$ was considered significant. Data were expressed as mean (± SD) in triplicate, and reproducibility was confirmed in three separate experiments.

Results

X-ray cocrystal structure. To compare the binding mode of the indenones with that of rosiglitazone, we determined the crystal structure of the ligand binding domain (LBD) of PPARγ complexed with rosiglitazone, KR-62776 or KR-62980. The cocrystal structures of the indenone revealed very different conformations compared to that of rosiglitazone. The head group of rosiglitazone stretched deep into the left stem of the cavity; however, the indenone moiety of KR-62776 and KR-62980 occupied the basal part while the side chain stretched deep into the upper part of cavity as shown in Figure 1. The binding mode of indenones, KR-62776 and KR-62980, is very similar that of GW0072, a partial agonist of PPARγ [11].

Morphological change in 3T3-L1 cells induced by indenone and rosiglitazone treatment. Although weight gain was observed in rosiglitazone-treated ob/ob mice, indenones did not cause weight gain [10]. Therefore, we measured the adipose conversion rates of 3T3-L1 preadipocyte cells caused by KR-62776 or rosiglitazone. When 3T3-L1 preadipocyte cells were treated with 1 μM of rosiglitazone, more than 80 % were converted to adipocyte cells. Approximately 5 % of the KR-62776-treated 3T3-L1 preadipocyte cells underwent differentiation (Fig. 2A). To test the effects of PPARγ agonists on differentiated 3T3-L1 cells, the differentiation-inducing agents IBMX cocktail and insulin were used to prepare differentiated cells. The differentiated 3T3-L1 adipocytes were treated with KR-62776, or rosiglitazone for three days. As was expected, no obvious morphological changes were observed in any of the cells (Fig. 2B).

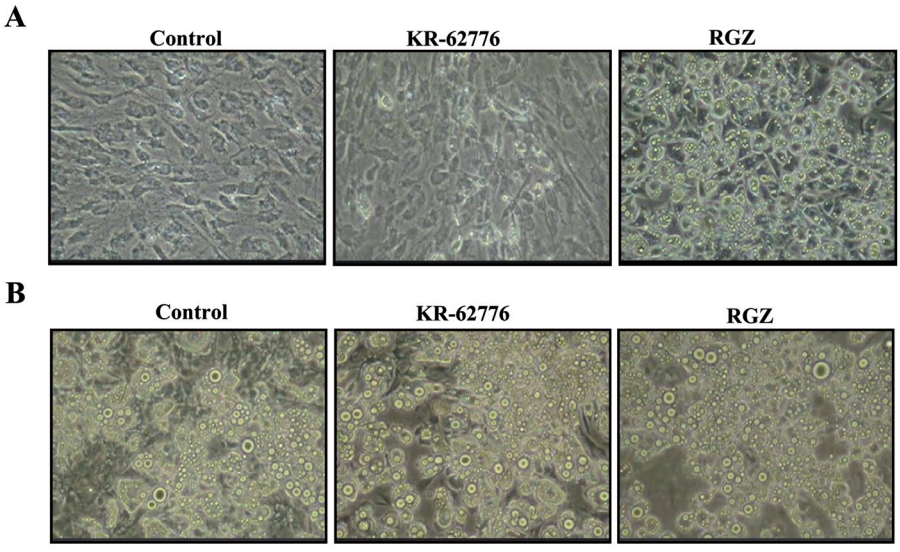

Figure 2. Effect of KR-62776 or rosiglitazone (RGZ) on adipogenic differentiation of 3T3-L1 Cells. (*A*) Postconfluent 3T3-L1 preadipocytes were incubated in DMEM culture medium containing 200 nM insulin with DMSO, 1 μM KR-62776 or 1 μM rosiglitazone for nine days. (*B*) Fully differentiated 3T3-L1 adipocytes were incubated in DMEM culture medium containing 200 nM insulin with DMSO, 1 μM KR-62776 or 1 μM rosiglitazone for three days.

This demonstrates that KR-62776, or rosiglitazone, does not alter the phenotype of differentiated cells within three days.

Proteomic profiling of KR-62776-treated and rosiglitazone-treated 3T3-L1 preadipocyte Cells. To identify proteins associated with phenotype changes (Fig. 2A), we compared the proteomic profiles of KR-62776- and rosiglitazone-treated 3T3-L1 preadipocytes (data not shown). No proteins related specifically to anti-diabetic activity were identified. However, structural proteins such as lamin A/C, vimentin, tubulin and actin, and the membrane trafficking associated protein TER ATPase, were strongly regulated by rosiglitazone. Because the phenotype of the cells was changed by rosiglitazone, it is thought that mainly differentiation-inducing proteins were changed on a large scale.

Proteomic profiling of KR-62776- or rosiglitazone-treated 3T3-L1 adipocyte cells. To understand the different biological activities, such as weight gain in the animal experiments, and to confirm the anti-diabetic activity of the two PPARγ agonists, the proteomic profiles of matched pairs of KR-62776- or rosiglitazone-treated 3T3-L1 adipocyte cells and non-treated adipocyte cells were analyzed (Fig. 3A–C). The proteomic analysis was carried out on total protein with p*I* values in the range of 3 – 10. Image pairs of gels from KR-62776- or rosiglitazone-treated adipocytes and control (non-treated) adipocytes were comparatively analyzed. From analysis of gel images, 53 spots corresponding to 42 proteins whose levels were altered more than 2.0-fold between KR-62776- or rosiglitazone-treated adipocytes and controls were identified (Fig. 3D–F). In KR-62776-treated 3T3-L1 adipocyte cells, 12 proteins were down-regulated and 24 proteins were up-regulated when compared to DMSO-treated cells as shown on the 'KR-62776 treated' gel. On the other hand, 12 proteins were down-regulated and 16 up-regulated in the rosiglitazone-treated adipocytes compared to DMSO-treated cells as shown on the 'RGZ treated' gel. Proteins, including hnRNP F, solute carrier family 25, p63, HSP60, DNA nucleotidylexotransferase, hnRNP H1, cGKI alpha, phosphodiesterase 6B, glucose-6-phosphate dehydrogenase, lamin A/C, TRPM7, pre-mRNA splicing factor 7, aldolase A, and aconitase 2, were up-regulated in both the KR-62776- and rosiglitazone-treated adipocytes. The expression of the five proteins tubulin apha 3, tubulin alpha 1, PRO1680, actin beta, and hnRNP A1 were decreased in both KR-62776- and rosiglitazone-treated adipocytes when compared to DMSO-treated adipocytes. The proteins separated by 2-DE and identified by MS are summarized in Table 1 and Figure 4.

The proteins up-regulated in both the KR-62776- and rosiglitazone-treated adipocytes, such as aconitase 2, aldolase A, and cGKI, were confirmed by literature reports to be strongly involved in glucose and fatty acid metabolism [23 – 25]. Therefore, the proteins up-regulated by the agonists confirmed the anti-diabetic effects of the compounds. One strongly up-regulated protein was a mitochondrial protein, aconitase 2, which appeared on the gel in four spots (8702, 8707, 8708, and 8709). All four spots were commonly increased in the KR-62776- and rosiglitazone-treated gels (Table 1), and spot 8213 was identified as another mitochondrial protein, aldolase A (accession no. 4557305). Expression of aldolase A was increased

Table 1. Differentially expressed proteins in 3T3-L1 adipocyte by KR-62776 or RGZ

Spot no.[a)]	Protein name	Changed pattern[b)] KR-62776 treated cell	RGZ treated cell	Accession no.[c)]	MOWSE Score	No. matched peptides	Theor. M_r (kDa)/pI[d)]	Seq. cov. (%)[e)]
0007	14-3-3 beta/alpha	Decreased	Increased	P31946	1.25e+004	6/25	27951/4.7	35
0106	SOX-13	Increased	n. s.	12643902	5.01e+008	18/21	98782/6.8	21
0107	annexin 5	Decreased	n. s.	4502107	1.88e+005	12/24	35805/4.9	38
0108	eIF 2C2	Increased	n. l.	19879661	2.83e+010	26/45	96799/9.3	37
0301	ACTB protein	Decreased	Decreased	15277503	5.695e+06	13 /21	41737/5.2	41
0705	gp96	Decreased	n. s.	4507677	7.622e+07	21 /51	92469/4.7	28
1010	FTCD	n. s.	Decreased	11140815	1.74e+006	10/20	58927/5.5	25
1105	ER60 precursor	Increased	n. s.	7437388	8.703e+04	10/17	56783/6.0	22
1405	proteasome 26S ATPase	n. s.	Decreased	5729991	1.74e+007	12/18	47366/5.0	35
1412	hnRNP F	Increased	Increased	4826760	1.67e+005	6/10	45672/5.3	25
1508	Tubulin alpha-3	Decreased	Decreased	6755901	4.41e+009	16/24	50136/4.9	44
1805	Hsp70 RY	n. s.	Increased	2135328	1.628e+05	12 /20	78996/5.1	23
2103	solute carrier family 25	Increased	Increased	55644901	2.738e+04	6/9	34062/9.9	28
2109	PP1 regulatory subunit 7 alpha2	Increased	Decreased	4633066	1.04e+004	6 /7	36838/5.1	29
2302	ACTB protein	Decreased	Decreased	15277503	4.38e+006	11/22	41737/5.2	43
2308	p63	Increased	Increased	2102667	1.43e+005	9/13	78151/8.5	12
2406	MMP-13	Decreased	n. s.	4505209	2.4e+006	12/20	53820/5.3	36
2503	Hsp60	Increased	Increased	31542947	2.36e+007	20/27	61055/ 5.7	45
2606	Hsp71	Increased	n. s.	24234686	1.35e+004	6/30	70898/5.3	13
2710	DNA nucleotidylexotransferase	Increased	Increased	29788762	1.1e+003	4/12	58437/8.5	10
3207	prolactin	Increased	n. s.	1620399	5.69e+003	7/14	25876/6.5	44
3309	hnRNP H1	Increased	Increased	5031753	2.34e+005	7/36	49229/5.8	26
3404	hnRNP H1	n. s.	Increased	5031753	1.389e+07	9 /17	49229/5.8	35
3606	4-PH alpha-1	Decreased	n. s.	4505565	1.18e+007	13/21	61049/5.7	25
4503	tubulin, alpha 1	Decreased	Decreased	57013276	8.6e+010	16 19	50152/4.9	46
5107	cGKI-alpha	Increased	Increased	6225588	1.01e+008	14/29	77804/5.2	25
5108	Phosphor-diesterase 6B	Increased	Increased	12652977	4.29e+004	11/15	98407/5.1	16
5510	Tubulin alpha	Increased	n. l.	6755901	2.29e+009	15/24	50152/4.9	41
5609	WD repeat-containing protein 1	Decreased	n. s.	12652891	5.46e+007	9/12	66194/6.1	27
6103	FXI	Increased	Decreased	4503627	1.76e+005	8/13	70109/8.4	18
6301	ARP1	n. s.	Decreased	5031569	1.17e+005	10/17	42614/6.1	42
6303	PRO1608	Decreased	Decreased	7770137	8.49e+005	9/13	50119/6.2	26
6407	fascin 1	n. l.	n. l.	4507115	1.62e+008	14/18	54399/6.8	40
6510	Glucose-6-phosphate dehydrogenase	Increased	Increased	12653141	4.84e+005	11/17	59257/6.4	20
6513	tubulin alpha 6	Increased	n. l.	14389309	3.42e+003	4/9	49895/4.9	13
7202	ERK2	n. s.	Decreased	20986531	1.26e+005	9/15	41390/6.5	24
7607	lamin A/C	Increased	Increased	27436946	1.42e+013	35/45	74140/6.5	49
8107	hnRNP A2/B1	n. s.	Decreased	4504447	3.42e+006	12/17	37430/8.9	36
8112	ANXA2	Increased	n. s.	18645167	1.45e+004	7/27	38473/7.5	25
8213	aldolase A	Increased	Increased	4557305	8.5e+003	4/10	39289/8.3	16
8312	TRPM7 protein	Increased	Increased	30046835	1.075e+05	9/15	62658/9.2	26
8608	pre-mRNA splicing factor 17	Increased	Increased	7706657	1.91e+005	12/18	65521/6.6	23

Table 1 *(Continued)*

Spot no.[a)]	Protein name	Changed pattern[b)] KR-62776 treated cell	RGZ treated cell	Accession no.[c)]	MOWSE Score	No. matched peptides	Theor. M_r (kDa)/pI[d)]	Seq. cov. (%)[e)]
8702	aconitase 2	Increased	Increased	5304852	1.49e+010	16/19	85426/7.3	27
8708	aconitase 2	Increased	Increased	4501867	1.45e+005	9/13	85426/7.3	14
9104	hnRNP A2/B1	Decreased	n. s.	4504447	2.12e+006	12/18	37430/8.9	47
9106	hnRNP A1	Decreased	Decreased	P09651	1.04e+004	5/16	38714/9.2	19

a) Spot numbers indicate the protein spot marked by 2-DE image software, PDQuest 7.1.0
b) Decreased or Increased indicates the proteins whose spot volumes were changed (positively or negatively) > 2.0-fold when analyzed on multiple gels (n = 3). n. s. = not significantly different; n. l. = not located in the same place on the 2-D-gel
c) Accession number in Swiss-Prot and NCBI database
d) Theoretical M_r (kDa)/pI
e) Sequence coverage % (MS data)

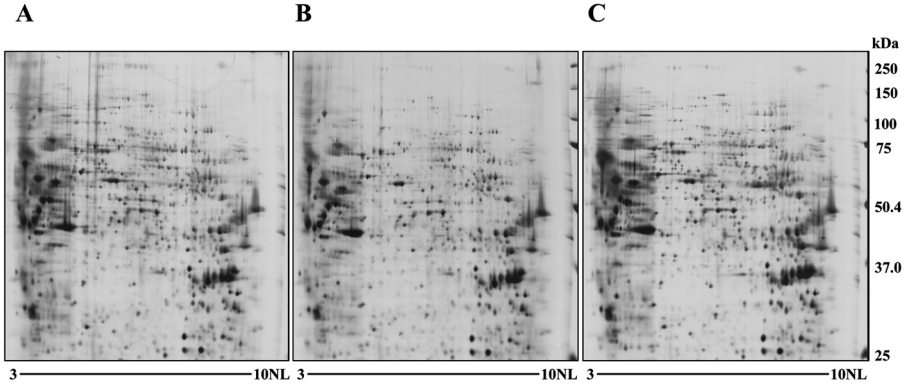

Figure 3. 2-DE images and comparative analysis of the expressed protein patterns between control, KR-62776-treated and rosiglitazone (RGZ)-treated 3T3-L1 adipocytes. 3T3-L1 preadipocytes cells were fully differentiated by treatment of IBMX cocktail. Then the fully differentiated 3T3-L1 cells were treated with (*A*) 0.1% DMSO + 200 nM insulin, (*B*) 200 nM insulin and 1 μM KR-62776, and (*C*) 200 nM insulin and 1 μM rosiglitazone for three days. Lysates from these treated cells were separated on a 2-D gel and then silver-stained for visualization of protein spots. To analyze the comparatively expressed protein patterns between 0.1% DMSO-, KR-62776- and rosiglitazone (RGZ)-treated 3T3-L1 adipocytes, the proteins were separated on a 2-D gel and then silver-stained for visualization of protein spots.

by 2.8-fold in KR-62776-treated cells and 4.9-fold in rosiglitazone-treated cells (Fig. 5A). Expression levels of cGMP-dependent protein kinase 1 (cGKI) were also enhanced by both KR-62776 (2.5-fold) and rosiglitazone (2.0-fold) as shown in Figure 5B. These data confirmed that KR-62776 and rosiglitazone have anti-diabetic effects.

One of the proteins (spot 3207) that was up-regulated 4.6-fold in KR-62776-treated cells, but did not significantly change in rosiglitazone-treated cells, was identified as prolactin (Fig. 5C, accession no. 1620399). Another interesting finding from the proteomic analysis is that ERK2 is differently regulated in the PPARγ agonist-treated 3T3-L1 cells. In the image analysis, spot 7202 (Fig. 5D) was identified as ERK2 and it was down-regulated over 9.0-fold in rosiglitazone-treated cells. However, the proteins were about 20% up-regulated in KR-62776-treated cells in comparison with control cells. 2-D gel was carried out three times to identify altered proteins by PPARγ agonists.

Western blotting of ERK and differentiation induced by the ERK inhibitor PD98059. As seen in previous studies, an activated PPARγ modulates transcription of target genes that are mainly involved in fatty acid and lipid metabolism in fat cells. Activated PPARγ also controls transcription of genes that are associated with the differentiation of fat cells [26]. However, activation of ERK signaling inhibits the activation of PPARγ through phosphorylation of PPARγ in adipocytes, thereby promoting lipolysis [27]. As mentioned, ERK is differentially expressed in KR-62776- and rosiglitazone-treated cells. Therefore, we focused on the expression level of the protein and the 2-DE data was confirmed by Western blotting. Phosphorylated ERK1/2 levels were mildly down-regulated in about 60% of rosiglitazone-treated differentiated cells in comparison with that of KR-62776-treated cells

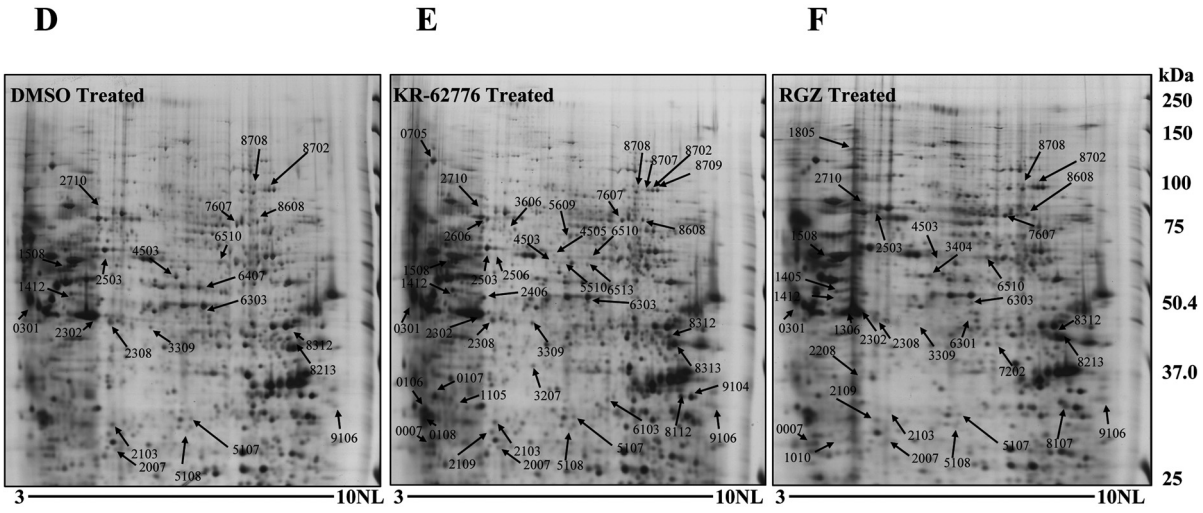

Figure 3. (*continued*) (*D*) Control (non-treated) 3T3-L1 cells; the arrows indicate commonly altered protein spots in the control gel compared with other gels. (*E*) 1 μM KR-62776-treated 3T3-L1 cells; the arrows indicate changed protein spots in the KR-62776-treated gel compared with the control gel. (*F*) 1 μM rosiglitazone-treated 3T3-L1 cells; the arrows indicate changed protein spots in the rosiglitazone-treated gel compared with the control gel. Numbers shown here are the same as those listed in supplement Table 1. Proteins shown are those that changed more than 2.0-fold in 3T3-L1 adipocytes by KR-62776 or rosiglitazone treatment. Protein spots were identified by MALDI-TOF MS.

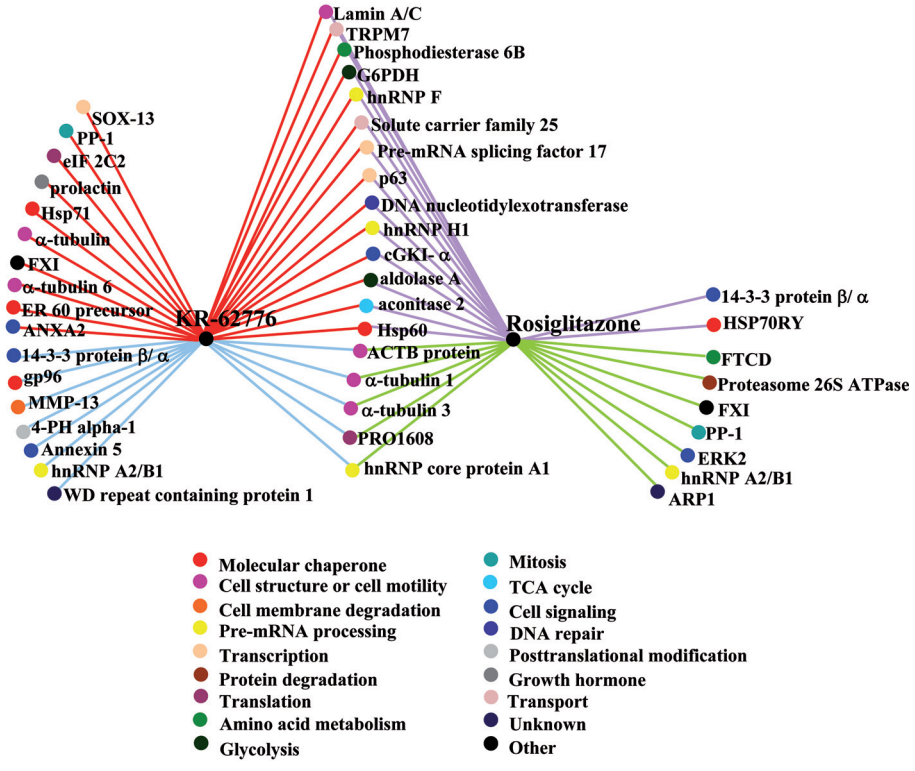

Figure 4. Proteins regulated in 3T3-L1 adipocytes by KR-62776 or rosiglitazone treatment.

(Fig. 6A). However, as shown in Figure 6B, after 14 days phosphorylated ERK1/2 was dramatically down-regulated in rosiglitazone-treated 3T3-L1 adipocyte cells and, conversely, strongly up-regulated in KR62776-treated adipocyte cells when compared to DMSO-treated controls. This suggests that KR-62776 induces the activation of ERK1/2 and rosiglitazone suppresses ERK1/2 activity. This means that the ERK pathway is involved in the differentiation of 3T3-L1 cells. Furthermore, the effect of ERK on the differentiation of the cells was tested using the ERK inhibitor PD98059. When 3T3-L1 preadipocyte cells were treated with PD98059 and either of the PPARγ agonists (rosiglitazone or KR-62776), a large propor-

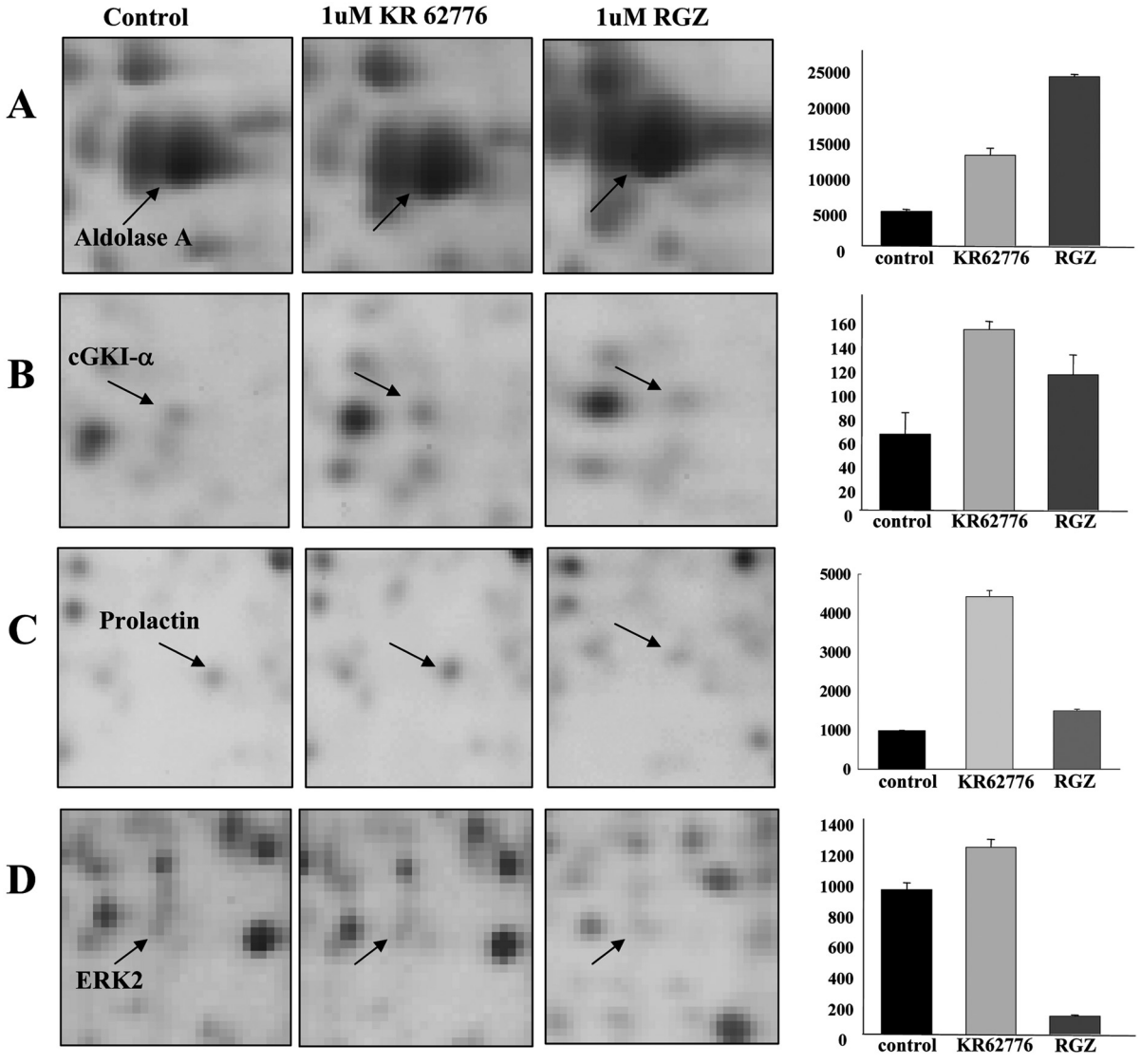

Figure 5. Close-up views of the regions of the 2-DE gels that show interesting differences in protein expression levels. (*A*) and (*B*) Commonly increased proteins in KR-62776 or rosiglitazone (RGZ)-treated 3T3-L1 adipocytes compared to control (non-treated 3T3-L1 adipocyte). (*C*) and (*D*) Differentially expressed proteins in KR-62776 or rosiglitazone treated 3T3-L1 adipocytes compared to controls (non-treated 3T3-L1 adipocyte). (*A*) aldolase A; (*B*) cGKI-α; (*C*) Prolactin; (D) ERK2. Histograms represent the mean ±SD of spot intensity (n = 3).

tion of the 3T3-L1 cells were converted to adipocytes (Fig. 6C, D).

Localization of PPARγ and phosphorylated PPARγ in 3T3-L1 cells. Several studies have shown that phosphorylation of PPARγ is an important factor in the regulation of PPARγ activity and the ERK/MAPK pathway is a key mediator of crosstalk between insulin signaling and PPARγ function. Activated ERK regulates PPARγ in a way that significantly reduces its transcriptional activity and ability to promote adipogenesis. ERK induces the phosphorylation of PPARγ on S84/S112 and this negatively regulates the activity of PPARγ [14, 28]. Interestingly, Burgermeister et al. report that the activity of PPARγ is regulated according to its subcellular localization [15]. The localization of PPARγ is mediated by direct MEK-PPARγ interaction. Mitogenic stimulation of the cells induces interaction between active nuclear MEK and PPARγ, followed by a rapid nuclear export of PPARγ, and a reduction in the transcriptional activity of PPARγ. Therefore, the ERK-activator MEK modulates activity of PPARγ through regulation of its subcellular localization.

In this experiment, KR-62776 up-regulates and activates ERK, but the amount of PPARγ is not changed in 2-D gel proteomic analysis. Therefore the subcellular localization of PPARγ and phosphorylated ERK

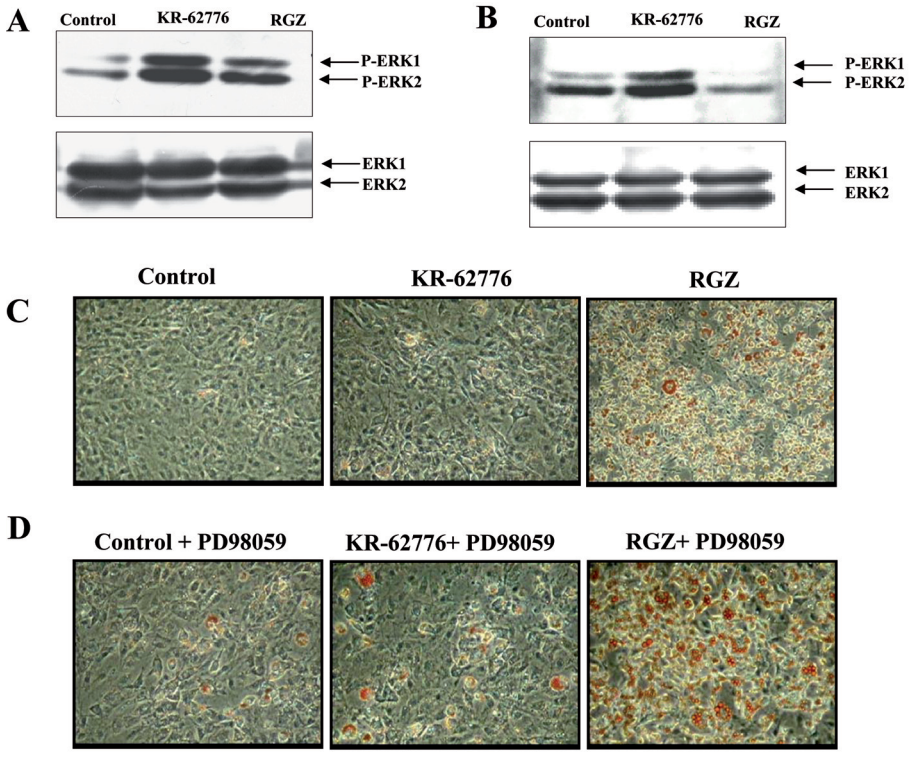

Figure 6. Western blotting of phospho-Erk1/2 and Microscopic observations of morphological changes induced by the ERK inhibitor PD98059. 20 micrograms of protein from untreated and KR-62776- or rosiglitazone (RGZ)-treated 3T3-L1 adipocytes were separated by 10% SDS-PAGE and transferred onto a PVDF membrane. Detection of the antigens was performed using the ECL method. Activated ERK1/2 was decreased by seven days of rosiglitazone treatment in 3T3-L1 cells (*A*) or by rosiglitazone treatment for 14 days in 3T3-L1 preadipocyte cells (*B*). Microscopic observations of morphological changes in 3T3-L1 cells treated with KR-62776 or rosiglitazone (RGZ) with or without the MAPK inhibitor PD98059. (*C*) 3T3-L1 preadipocytes were stimulated by DMSO (0.1%), KR-62776 or rosiglitazone (1 μM), with 200 nM insulin. (*D*) 3T3-L1 preadipocytes were stimulated by DMSO (0.1%), KR-62776 or rosiglitazone (1 μM), with 200 nM insulin and PD98059 (10 μM). After seven days, cells were stained with Oil-Red O. Lipid droplet showed orange colors.

was observed. To verify that KR-62776 induced relocalization of PPARγ the protein was examined by confocal fluorescence microscopy. When 3T3-L1 cells were treated with DMSO or rosiglitazone, PPARγ was mainly localized in the nucleus. However, PPARγ nuclear fluorescence was reduced in KR-62776-treated cells (Fig. 7A). A large amount of ERK1/2 was detected in the nucleus of KR-62776-treated cells compared to rosiglitazone-treated cells (Fig. 7B). MEK was also localized in the nucleus of KR-62776-treated cells as compared to rosiglitazone-treated cells. Lipid droplets were formed during the process of adipogenesis in rosiglitazone-treated 3T3-L1 cells (data not shown).

Western blot analysis with cytosolic and nuclear fractions of 3T3-L1 cells demonstrated that PPARγ was slightly increased by KR-62776, but not rosiglitazone, in cytosolic fractions, while PPARγ was decreased by KR-62776 more than rosiglitazone in the nuclear fraction (Fig. 7C). The expression levels of PPARγ increased in the cytosolic fraction but decreased in the nuclear fraction because PPARγ export into the cytosol correlated with the presence phosphorylated ERK1/2 and this was activated by KR-62776. The intensity of ERK and phosphorylated ERK cytosolic labeling was indistinguishable by Western blot analysis. However, phosphorylation of ERK1/2 in the nucleus was dramatically decreased by rosiglitazone- but increased by KR-62776-treatment (Fig. 7C). It was reported that activation of ERK signaling inhibits the activation of PPARγ through phosphorylation of PPARγ in adipocytes [27]. Therefore the level of phosphorylated PPARγ in PPARγ agonist-treated 3T3-L1 cells was measured by Western blot analysis and it was found that phospho-PPARγ was dramatically decreased in rosiglitazone-treated 3T3-L1 cells (Fig. 7D). These results show that KR-62776 activates MEK and ERK1/2, but inhibits transcriptional activity of PPARγ and reduces adipogenesis of 3T3-L1 cells through a mechanism that includes export of PPARγ from the nucleus into the cytoplasm.

To identify molecular alterations of the PPARγ agonists on adipocyte differentiation in the 3T3-L1 cells, we also examined gene expression profiles of adipogenesis related genes induced by RGZ or KR-

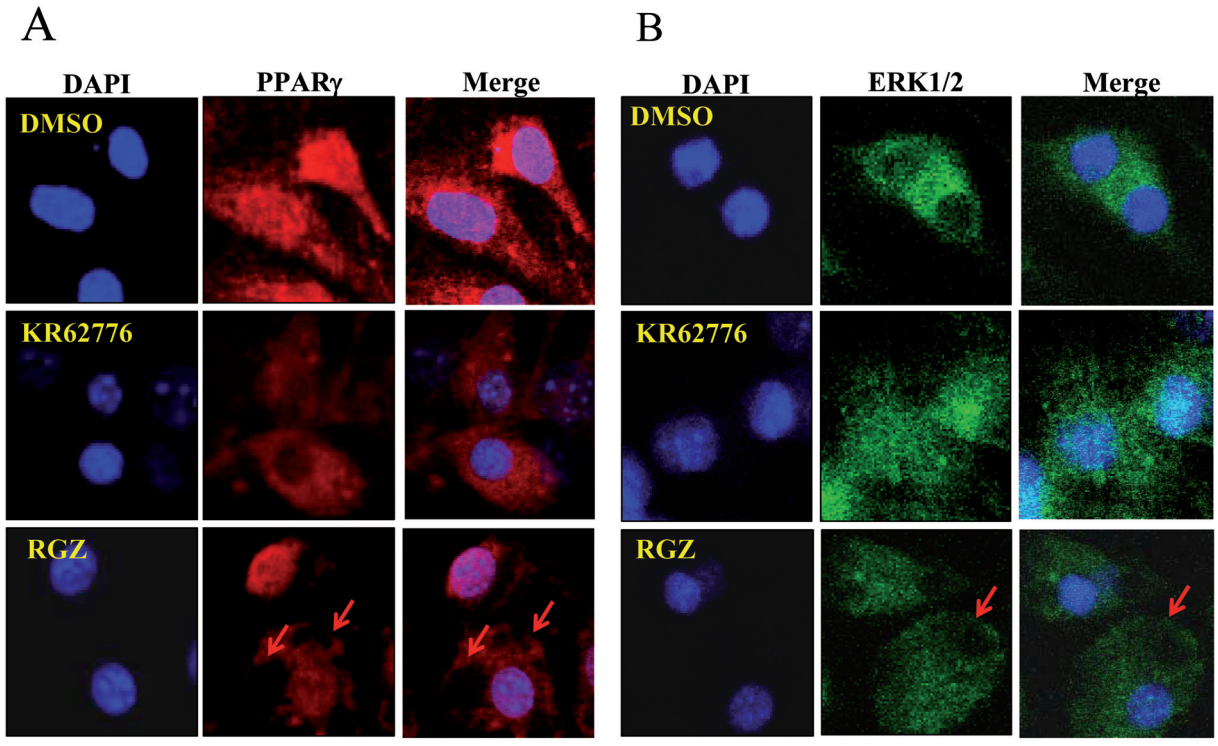

Figure 7. Localization of PPARγ and Erk1/2 in 3T3-L1 cells. Cells were grown on coverslips and treated with KR-62776 or rosiglitazone (RGZ) for nine days. PPARγ are labeled in red whereas ERK1/2 is labeled in green. Nuclei were visualized with DAPI staining. Immunofluorescence microscopy revealed that PPARγ translocated from the nucleus to cytosol by KR-62776 (*A*). Distribution of Erk1/2 (*B*) was more condensed in the nucleus than in the cytosol by KR-62776.

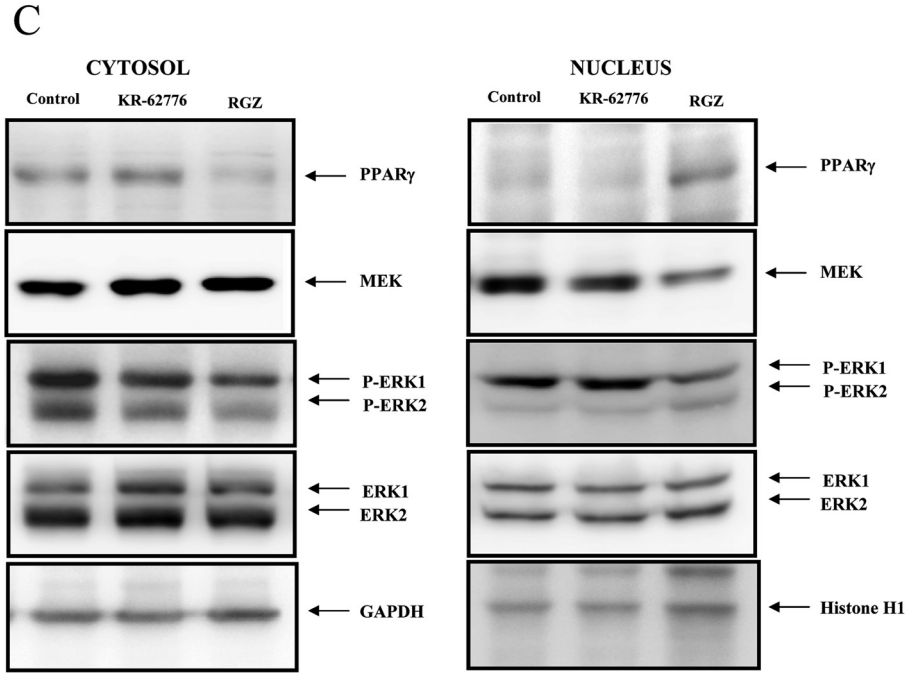

Figure 7. (*continued*) (*C*) Verification of the localization of PPARγ, Erk1/2 and MEK using Western blot analysis.

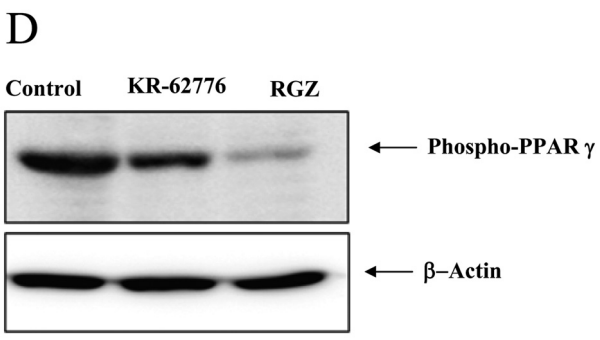

Figure 7. (*continued*) (*D*) Verification of phosphorylation of PPARγ using Western blot analysis. 3T3-L1 preadipocyte cells were treated with DMSO, 1 μM KR-62776 or 1μM rosiglitazone with 200 nM insulin for 12 days. Phosphorylated PPARγ was decreased by treatment of rosiglitazone compared with DMSO or KR-62776.

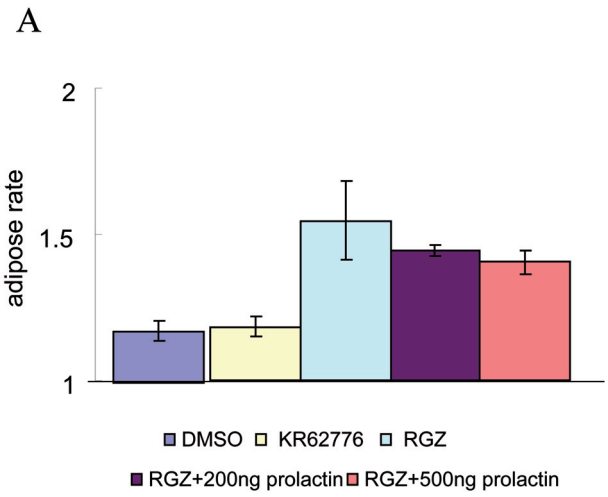

Figure 8. Differentiation of 3T3-L1 preadipocyte cells was decreased by prolactin treatment. 3T3-L1 preadipocyte cells were treated with 1 μM KR-62776, 1 μM KR-62980, 1μM rosiglitazone or 1μM rosiglitazone + prolactin with 200 nM insulin for nine days. The cells were fixed with formaldehyde and stained with the lipophilic dye, Oil-Red O. The dye retained from the lipid vacuoles was measured by determination of the optical density at 540 nm and shown on the y-axis (mean ±SD).

62776 in adipocytic cells using microarray experiments. In the RGZ-treated preadipocytic cells, adipogenesis related genes, such as Facl2, Lpl, Acdc (also called Acrp30), and Fabp4 **(**aP2) genes, were up-regulated, whereas the genes in KR-62776-treated cells were moderately regulated (data not shown).

Inhibition of differentiation by prolactin. Prolactin is expressed in human preadipocytes and its expression decreases progressively throughout adipogenesis. Ciglitazone, one of glitazones, suppressed the expression of prolactin mRNA [29]. As shown Figure 5C, prolactin expression was down-regulated by rosiglitazone and up-regulated by KR-62776 in 2-D gel experiments. To test the effect of prolactin on adipogenesis, 3T3-L1 preadipocytes were treated with a common differentiation protocol. Morphological conversion was verified by lipid accumulation, as seen by Oil-Red O staining. Co-incubation of prolactin with rosiglitazone very mildly suppressed the morphological conversion in a dose-dependent manner (Fig. 8 A and B). However, KR-62776 treatment did not change the cellular phenotype (Fig. 8 B).

Discussion

The 2-DE technique was used to profile proteins that were differentially expressed between KR-62776- and rosiglitazone-treated 3T3-L1 adipocyte cells. Fifty-three spots corresponding to 42 proteins were altered more than 2.0-fold between KR-62776- or rosiglitazone-treated adipocytes when compared to DMSO-treated control cells. In this study, we found that the mitochondria proteins such as aldolase A and aconitase 2 were up-regulated by KR-62776 and rosiglitazone in 3T3-L1 adipocyte cells. Aldolase A is well known as a glycolytic enzyme and previous studies demonstrated a significant co-localization of aldolase and GLUT4 in 3T3-L1 adipocyte cells [24]. GLUT4, up-regulated by KR-62776 and rosiglitazone in 3T3-L1 adipocyte cells, itself migrates to plasma membrane from intracellular sites and promotes glucose uptake [5]. Aconitase 2 was also commonly up-regulated in KR-62776- or rosiglitazone-treated cells. Aconitase 2 is a mitochondrial protein and it is involved in fatty acid metabolism. Mitochondria are not only the major site of fatty acid oxidation in cells, but also may play a critical role in lipogenesis [30]. It has been reported that insulin sensitizer enhances adipocyte differentiation and mitochondria biogenesis [23]. Therefore, up-regulation of mitochondrial proteins involved in fatty acid metabolism and lipogenesis is one of the key functions of the PPARγ agonists, and that is an important factor for understanding the anti-diabetic activity of the agonists. These results suggest that the agonists of PPARγ, which bind to the protein using a different binding pocket, show anti-diabetic effects via up-regulation of the proteins such as aconitase 2, aldolase and GLUT4, etc.

2-DE gel analysis also shows that expression of cGKI was enhanced by KR-62776 and rosiglitazone, which was interesting because of a report that cGKI enhanced PPARγ expression levels and caused activation of the phosphatidylionsitol 3-kinase/Akt signaling pathway [25]. PI3K activity is necessary for insulin-stimulated glucose uptake [30]. KR-62776 and

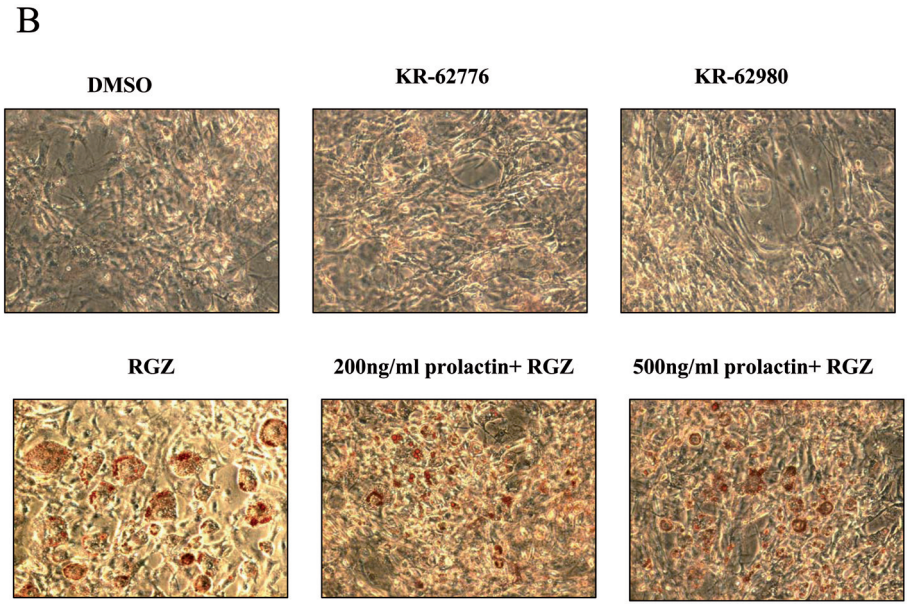

Figure 8. (*continued*)

rosiglitazone lead to increased expression of the protein that plays an important role in glucose utilization.

As already mentioned, PPARγ is a ligand-activated transcription factor of the nuclear receptor superfamily that regulates genes involved in differentiation, metabolism and immunity. As a central regulatory component, PPARγ activity is well controlled during various cellular processes; indeed, mitogenic stimulation often suppresses PPARγ's transcriptional activity. This down-regulation is mediated largely by the ERK/MAPK signaling cascade, which attenuates PPARγ's transactivation function either by inhibitory phosphorylation or by modulating PPARγ's nucleo-cytoplasmic localization [31]. An interesting point is that KR-62776, one of the PPARγ agonists, up-regulated ERK activity. Alteration of the amount of phosphorylated ERK1/2 was confirmed by Western blotting. However, Park et al. reported that KR-62776 inhibited RANKL-induced phosphorylation of p38MAPK, ERK, and JNK in osteoclast differentiation [32]. This result also supports that PPARγ may modulate the MAP kinase signaling pathway.

The localization of PPARγ and ERK1/2 was also observed using confocal microscopy. These results are very important to explain why KR-62776 does not induce differentiation of preadipocytes and does not stimulate weight gain in animals, even though it is a potential PPARγ agonist. The changes in the subcellular localization of PPARγ may also represent a novel strategy for selective interference in patients with proliferation-related diseases. According to reports, the MEK/ERK signaling pathway regulates the expression of C/EBPα and PPARγ during the adipogenesis of 3T3-L1 cells [33]. Therefore, the modulation of ERK activity might be involved in differentiation of adipocyte tissues through the regulation of nucleo-cytoplasmic compartmentalization of PPARγ.

It has been reported that prolactin, up-regulated by KR-62776 treatment, regulates the levels of C/EBPβ and PPARγ mRNA [34]. Differentiation of 3T3-L1 cells induced by rosiglitazone was mildly suppressed by prolactin (Fig. 8). However, the mode of prolactin action in adipogenesis is not clear. These results suggest that prolactin is one of the factors that regulates the morphological conversion of preadipocytes and is also involved in the inhibition of the adipogensis by indenones, the new PPARγ agonists. In conclusion, the protein expression profiles of 3T3-L1 adipocytes were observed in KR-62776- or rosiglitazone-treated adipocytes, using 2-DE. Proteomic profiling demonstrated that the proteins with the most common expression changes caused by the PPARγ agonists were also strongly related to anti-diabetic effects. We also found that the phosphorylation of ERK was decreased in rosiglitazone-treated 3T3-L1 adipocyte cells, while phosphorylated ERK and prolactin expression were increased in KR-62776-treated cells. These data explain why the biological activity of KR-62776 has anti-diabetic activity but does not induce obesity. This indicates that suppression of weight gain following treatment with KR-62776 is due partly to the synergistic effects of various proteins, including the phosphorylation of ERK, the expression of prolactin and other signaling molecules

in tissues. Here, we provide a mechanistic explanation for the different and common biological activities of the two-types of PPARγ agonists, each with different chemical structures, using 2-DE and MALDI-TOF MS technology. We believe that the chemical proteomic approach may be a potentially useful method for revealing novel mechanisms of active compounds or drugs with unknown cellular function. The binding modes of the PPARγ agonists might be one of the important factors in understanding the biological mechanism of the agonists on the transcription factors.

Acknowledgments. This work was supported by a grant from the center for biological modulators of the 21st Century Frontier Research Program (CBM1-B500-001-1-00).

1 Shih, D. Q. and Stoffel, M. (2002) Molecular etiologies of mody and other early-onset forms of diabetes. Current Diabetes Report 2, 125–134.
2 MacDougald, O. A. and Lane, M. D. (1995) Transcriptional Regulation of Gene Expression During Adipocyte Differentiation. Ann. Rev. Biochem. 64, 345–373.
3 Ricote, M., Li, A. C., Willson, T. M., Kelly, C.J. and Glass, C. K. (1998) The peroxisome proliferator-activated receptor-gamma is a negative regulator of macrophage activation. Nature 391, 79–82.
4 Lehmann, J. M., Moore, L. B., Smith-Oliver, T. A., Wilkison, W. O., Wilkison and T. M., Kliewer, S. A. (1995) An Antidiabetic thiazolidinedione is a high affinity ligand for peroxisome proliferator-activated receptor gamma. J. Biol. Chem. 270, 12953–12956.
5 Saltiel, A. and Olefsky, J. M. (1996) Thiazolidinediones in the treatment of insulin resistance and type 2 diabetes. Diabetes; 45, 1661–1669.
6 Olefsky, J. M. (2000) Treatment of insulin resistance with peroxisome proliferator–activated receptor γ agonists. J. Clin. Invest. 106, 467–472.
7 Cavaghan, M. K., Ehrmann, D. A. and Polonsky, K. S. (2000) Interactions between insulin resistance and insulin secretion in the development of glucose intolerance. J. Clin. Invest. 106, 329–333.
8 Kletzien, R. F., Clarke, S. D. and Ulrich, R. G. (1992) Enhancement of adipocyte differentiation by an insulin-sensitizing agent. Mol. Pharm. 41, 393–398.
9 Ahn, J. H., Shin, M. S., Jung, S. H., Kim, J. A., Kim, H. M., Kim, S. H., Kang, S. K., Kim, K. R., Rhee, S. D., Park, S. D., Lee, J. M., Lee, J. H., Cheon, H. G. and Kim, S. S. (2007) Synthesis and structure–activity relationship of novel indene N-oxide derivatives as potent peroxisome proliferator activated receptor γ (PPARγ) agonists. Bioorg. Med. Chem. Lett. 17, 5239–5244.
10 Kim, K. R., Lee, J. H., Kim, S. J., Rhee, S. D., Jung, W. H., Yang, S. D., Kim, S. S., Ahn, J. H. and Cheon, H. G. (2006) KR-62980: a novel peroxisome proliferator-activated receptor gamma agonist with weak adipogenic effects. Biochem. Pharm. 72, 446–454.
11 Oberfield, J. L., Collins, J. L., Holmes, C. P., Goreham, D. M., Cooper, J. P., Cobb, J. E., Lenhard, J. M., Hull-Ryde, E. A., Mohr, C. P., Blanchard, S. G., Parks, D. J., Moore, L. B., Lehmann, J. M., Plunket, K., Miller, A. B., Milburn, M. V., Kliewer, S. A. and Willson, T. M. (1999) A peroxisome proliferator-activated receptor gamma ligand inhibits adipocyte differentiation. Proc. Natl. Acad. Sci. USA 96, 6102–6106.
12 Wright, H. M., Clish, C. B., Mikami, T., Hauser, S., Yanagi, K., Hiramatsu, R., Serhan, C. N. and Spiegelman, B. M. (2000) A synthetic antagonist for the peroxisome proliferator-activated receptor gamma inhibits adipocyte differentiation. J. Biol. Chem. 275, 1873–1877.
13 Mukherjee, R., Hoener, P. A., Jow, L., Bilakovics, J., Klausing, K., Mais, D. E., Faulkner, A., Croston, G. E. and Paterniti, J. R. (2000) A Selective Peroxisome Proliferator-Activated Receptor-γ (PPARγ) Modulator Blocks Adipocyte Differentiation but Stimulates Glucose Uptake in 3T3-L1 Adipocytes. Mol. Endo. 14, 1425–1433.
14 Hu, E., Kim, J. B., Sarraf, P. and Spiegelman, B. M. (1996) Inhibition of Adipogenesis Through MAP Kinase-Mediated Phosphorylation of PPARγ. Science **274**, 2100–2103.
15 Burgermeister, E., Chuderland, D., Hanoch, T., Meyer, M., Liscovitch, M. and Seger, R. (2007) Interaction with MEK causes nuclear export and downregulation of peroxisome proliferator-activated receptor gamma. Mol. Cell. Biol. 27, 803–817.
16 Uppenberg, J., Svensson, C., Jaki, M., Bertilsson, G., Jendeberg, L. and Berkenstam, A. (1998) Crystal structure of the ligand binding domain of the human nuclear receptor PPAR-gamma. J. Biol. Chem. 273**,** 31108–31112.
17 Leslie, A. G. (1999) Integration of macromolecular diffraction data. Acta Crystallogr. D Biol. Crystallogr. 55**,** 1696–702.
18 Jones, T. A., Zou, J-. Y., Cowan, S. W. and Kjeldgaard, M. (1991) Improved methods for building protein models in electron density maps and the location of errors in these models. Acta Crystallogr. A 47**,** 110–119.
19 Green, H. and Kehinde, O. (1975) An established preadipose cell line and its differentiation in culture. II. Factors affecting the adipose conversion. Cell 5, 19–27.
20 Görg, A., Obermaier, C., Boguth, G., Harder, A., Scheibe, B. R., Wildgruber, R. W. and Weiss, W. (2000) The current state of two-dimensional electrophoresis with immobilized pH gradients. Electrophoresis 21, 1037–1053.
21 Jensen, O. N., Wilm, M., Shevchenko, A. and Mann, M. (1999) Sample preparation methods for mass spectrometric peptide mapping directly from 2-DE gels. Methods Mol. Biol. 112, 513–530.
22 Meunier, C., Bordereaux, D., Porteu, F., Gisselbrecht, S., Chretien, S. and Courtois, G. (2002) Cloning and characterization of a family of proteins associated with Mpl. J. Biol. Chem. 277, 9139–9147.
23 Wilson-Fritch, L., Burkart, A., Bell, G., Mendelson, K., Leszyk, J., Nicoloro, S., Czech, M. and Corvera, S. (2003) Mitochondrial biogenesis and remodeling during adipogenesis and in response to the insulin sensitizer rosiglitazone. Mol. Cell. Biol. 23, 1085–1094.
24 Kao, A. W., Noda, Y., Johnson, J. H., Pessin, J. E. and Saltiel, A. R. (1999) Aldolase mediates the association of F-actin with the insulin-responsive glucose transporter GLUT4. J. Biol. Chem. 274**,** 17742–17747.
25 Wolfsgruber, W., Feil, S., Brummer, S., Kuppinger, O., Hofmann and F., Feil, R. (2003) A proatherogenic role for cGMP-dependent protein kinase in vascular smooth muscle cells. Proc. Natl. Acad. Sci. USA 100, 13519–13524.
26 Spiegelman, B. M. and Flier, J. S. (1996) Adipogenesis and obesity: rounding out the big picture. Cell 87, 377–389.
27 Camp, H. S. and Tafuri, S. R. (1997) Regulation of peroxisome proliferator-activated receptor gamma activity by mitogen-activated protein kinase. J. Biol. Chem. 272**,** 10811–10816.
28 Diradourian, C., Girard, J. and Pegorier, J. P. (2005) Phosphorylation of PPARs: from molecular characterization to physiological relevance. Biochimie 87, 33–38.
29 McFarland-Mancini M., Hugo E., Loftus J. and Ben-Jonathan N. (2006) Induction of prolactin expression and release in human preadipocytes by cAMP activating ligands. Biochem. Biophys. Res. Comm. 344, 9–16.
30 Czech, M. P. and Corvera, S. (1999) Signaling mechanisms that regulate glucose transport. J. Biol. Chem. 274**,** 1865–1868.
31 31.Burgermeister, E. and Seger, R. (2007) MAPK- Kinases as Nucleo-Cytoplasmic Shuttles for PPARγ. Cell Cycle 6, 1539–1548.
32 Park, J. Y., Bae, M. A., Cheon, H. K., Kim, S. S., Hong, J. M., Kim, T. H., Choi, J. Y., Kim, S. H., Lim, J., Choi, C. H., Shin, H. I., Kim, S. Y. and Park, E. K. (2008) A novel PPARc agonist,

KR62776, suppresses RANKL-induced osteoclast differentiation and activity by inhibiting MAP kinase pathways. Biochem. Biophys. Res. Comm. 378, 645–649.

33 Prusty, D., Park, B. H., Davis, K. E. and Farmer, S. R. (2002) Activation of MEK/ERK signaling promotes adipogenesis by enhancing peroxisome proliferator-activated receptor gamma and C/EBPalpha gene expression during the differentiation of 3T3-L1 preadipocytes. J. Biol. Chem. 277**,** 46226–4632.

34 Nanbu-Wakao, R., Fujitani, Y., Masuho, Y., Muramatu, M. and Wakao, H. (2000) Prolactin enhances CCAAT enhancer-binding protein-beta and peroxisome proliferator-activated receptor gamma messenger RNA expression and stimulates adipogenic conversion of NIH-3T3 cells. Mol. Endocrinol. 14, 307–316.